

are clearly displaced from each other by several arcseconds along the slit. This displacement is seen both at the jet source and at the positions on either side. In terms of the model sketched in Fig. 2a, the reversed blue and red shifts would be due to a reversal of the jet's east–west orientation with respect to the line of sight and the displacement along the slit corresponds to a marked tilt of the projected jet axis with respect to the north–south direction. Again the blue stream, indicating material flowing out of the solar surface, extends to almost 3.3 arcsec away from the source whereas the red stream, although brighter, is only seen 1.1 arcsec from the centre.

The observation that explosive events are bi-directional jets provides new evidence that they result from magnetic reconnection above the solar surface. From simultaneous magnetic field and ultraviolet measurements Dere *et al.*<sup>18</sup> note that explosive events are often found on the chromospheric network boundary and seem to be associated with the cancellation of photospheric magnetic fields. The network consists of curtains of very strong magnetic flux tubes. All flux tubes are anchored by their footpoints to the photosphere. The continual motions in the photosphere mean that field lines of opposite polarity are naturally drawn together. If flux tubes with opposite-polarity field lines are pushed together a current sheet forms. In a finite-resistivity plasma, a small region near the neutral line may collapse and create a thin reconnection region. From this region, plasma is ejected in both directions along the field lines with a velocity of the order of the Alfvén speed<sup>11,12</sup> (Fig. 2b). If there is an obstacle blocking one side, the situation is not as idealized in Fig. 2, and the flow may be uni-directional. For example, jets directed out of the Sun may stream freely up to coronal heights whereas the downward flow could quickly be slowed down by the increasing density of the chromosphere. This would in a simple manner explain the larger spatial extent of the blue-shifted wing in our observations.

The observations presented here seem to establish the association between bi-directional jets and reconnection. Since the launch of SUMER, a vast collection of data on explosive events has been accumulated. We expect that similar bi-directional jets are to be seen at and above active regions wherever reconnection occurs. The present and future observations of this kind will lead to a better understanding of how the Sun's magnetic energy feeds its hot corona and the solar wind. □

Received 14 November 1996; accepted 7 March 1997.

1. Giovanelli, R. G. A theory of chromospheric flares. *Nature* **158**, 81–82 (1946).
2. Gold, T. & Hoyle, F. Solar flares. *Mon. Not. R. Astron. Soc.* **120**, 89–105 (1960).
3. Priest, E. R. *Solar Flare Magnetohydrodynamics* (Gordon & Breach, London, 1981).
4. Hundhausen, A. J. in *Proc. 6th Int. Solar Wind Conf.* (eds Pizzo, V. J., Holzer, T. E. & Sime, D. G.) 181–214 (Nat. Center for Atmospheric Res., Boulder, 1988).
5. Gold, T. in *AAS-NASA Symp. on Solar Flares* (ed. Hess, W. N.) 389–395 (NASA-SP 50, NASA, Washington DC, 1964).
6. Axford, W. I. & McKenzie, J. F. in *Solar Wind Seven 1–5* (eds Marsch, E. & Schwenn, R.) (Pergamon, Oxford, 1992).
7. Tsuneta, S. *et al.* Global restructuring of the coronal magnetic fields observed with the Yohkoh soft X-ray telescope. *Publ. Astron. Soc. Jpn.* **44**, L211–L214 (1992).
8. Masuda, S. *et al.* A loop-top hard X-ray source in a compact solar flare as evidence for magnetic reconnection. *Nature* **371**, 495–497 (1994).
9. Porter, J. G. *et al.* Microflares in the solar magnetic network. *Astrophys. J.* **323**, 380–390 (1987).
10. Webb, D. F. *et al.* The correspondence between X-ray bright points and evolving magnetic features in the quiet Sun. *Solar Phys.* **144**, 15–35 (1993).
11. Petschek, H. E. in *AAS-NASA Symp. on Solar Flares* (ed. Hess, W. N.) 425–437 (NASA-SP 50, NASA, Washington DC, 1964).
12. Priest, E. R. *Solar Magnetohydrodynamics* (Reidel, Norwell, MA, 1982).
13. Rabin, D. & Dowdy, J. F. Ir Pervasive variability in the quiet solar transition region. *Astrophys. J.* **398**, 665–681 (1992).
14. Brueckner, G. E. & Bartoe, J.-D.F. Observations of high-energy jets in the corona above the quiet Sun, the heating of the corona, and the acceleration of the solar wind. *Astrophys. J.* **272**, 329–348 (1983).
15. Dere, K. P., Bartoe, J.-D.F. & Brueckner, G. E. Explosive events in the solar transition zone. *Solar Phys.* **123**, 41–68 (1989).
16. Dere, K. P. Explosive events, magnetic reconnection, and coronal heating. *Adv. Space Res.* **14**, 13–22 (1994).
17. Brueckner, G. E. *et al.* HRTS results from Spacelab 2. *Adv. Space Res.* **6**, 263–272 (1986).
18. Dere, K. P. *et al.* Explosive events and magnetic reconnection in the solar atmosphere. *J. Geophys. Res.* **96**, 9399–9407 (1991).
19. Wilhelm, K. *et al.* SUMER—solar ultraviolet measurements of emitted radiation. *Solar Phys.* **162**, 189–231 (1995).
20. Wilhelm, K. *et al.* First results of the SUMER telescope and spectrometer—solar ultraviolet measurements of emitted radiation—on SOHO: I. Spectra and spectrodiometry. *Solar Phys.* (in the press).

21. Lemaire, P. *et al.* First results of the SUMER telescope and spectrometer—solar ultraviolet measurements of emitted radiation—on SOHO: II. Imagery and data management. *Solar Phys.* (in the press).
22. Dere, K. P. *et al.* UV observations of macrospicules at the solar limb. *Solar Phys.* **119**, 55–63 (1989).

**Acknowledgements.** We thank J. Kimchuk for advice on the presentation of this work. The SUMER project is supported by DARA, CNES, NASA and the ESA PRODEX programme (Swiss contribution). SUMER is part of SOHO, the Solar and Heliospheric Observatory, of ESA and NASA.

Correspondence should be addressed to D.E.I. (e-mail: innes@linmpi.mpa.gwdg.de).

## An X-ray-induced insulator–metal transition in a magnetoresistive manganite

V. Kiryukhin\*, D. Casa\*, J. P. Hill†, B. Keimer\*, A. Vigliante‡, Y. Tomioka‡ & Y. Tokura‡§

\* Department of Physics, Princeton University, Princeton, New Jersey 08544, USA

† Department of Physics, Brookhaven National Laboratory, Upton, New York 11973, USA

‡ Joint Research Center for Atom Technology (JRCAT), Tsukuba, Ibaraki 305, Japan

§ Department of Applied Physics, University of Tokyo, Tokyo 113, Japan

Manganese oxides of the general formula  $A_{1-x}B_xMnO_3$  (where A and B are trivalent and divalent cations, respectively) have recently attracted considerable attention by virtue of their unusual magnetic and electronic properties<sup>1–9</sup>. For example, in some of these materials magnetic fields can drive insulator-to-metal transitions where both the conductivity and magnetization change dramatically—an effect termed ‘colossal magnetoresistance’<sup>1–3</sup>—raising hopes for application of these materials in the magnetic recording industry<sup>1–9</sup>. Here we show that in one such compound,  $Pr_{0.7}Ca_{0.3}MnO_3$ , a transition from the insulating antiferromagnetic state to the metallic ferromagnetic state can be driven by illumination with X-rays at low temperatures (<40 K). This transition is accompanied by significant changes in the lattice structure, and can be reversed by thermal cycling. This effect, undoubtedly a manifestation of the strong electron–lattice interactions believed to be responsible for the magnetoresistive properties of these materials<sup>6–9</sup>, provides insights into the physical mechanisms of persistent photoconductivity, and may also find applications in X-ray detection and X-ray lithographic patterning of ferromagnetic nanostructures.

The  $x = 0$  and  $x = 1$  end-members of the  $Pr_{1-x}Ca_xMnO_3$  family are insulating antiferromagnets with the manganese ion in the  $Mn^{3+}$  and  $Mn^{4+}$  valence states, respectively<sup>10</sup>. For intermediate  $x$ , the average Mn valence is non-integer and the material is generally semiconducting or metallic at high temperatures. At low temperatures, the charge carriers localize in a variety of structural and magnetic ordering patterns with mixed valences of the manganese ions<sup>10</sup>. The charge ordering is associated with lattice distortions which can be revealed by X-ray and neutron diffraction. In  $Pr_{0.7}Ca_{0.3}MnO_3$  this metal–insulator transition occurs at temperature  $T \approx 200$  K (ref. 3), and the low-temperature charge-ordering pattern<sup>4,10</sup> is sketched in the inset of Fig. 1. Note that this pattern (doubling of the unit cell in one lattice direction) is commensurate with the underlying nearly-cubic lattice despite the incommensurate average Mn valence. The low-temperature magnetic structure is antiferromagnetic with a weak uncompensated moment due to spin canting<sup>4</sup>. The material can be driven back into the metallic state by applying a critical magnetic field  $H_c$ ;  $H_c \approx 4T$  at low temperatures<sup>3,4</sup>. The metallic state is ferromagnetic due to double exchange<sup>4</sup>. This field-induced transition is associated with large hysteresis; the material in fact remains metallic after the field is reduced to zero, but reverts to the charge-ordered state on subse-

quent heating above 60 K. Similar metastability phenomena have also been observed in other manganites<sup>5</sup>.

The intensity of a Bragg reflection characteristic of the low-temperature charge-ordered structure, (4, 1.5, 0), was monitored by neutron diffraction from a single-crystal sample and is shown in Fig. 1 as a function of temperature. (The reflections are indexed on an orthorhombic, though nearly cubic, lattice with lattice constants  $a = 5.426 \text{ \AA}$ ,  $b = 5.478 \text{ \AA}$  and  $c/\sqrt{2} = 5.430 \text{ \AA}$ ; ref. 10.) The temperature dependence of the intensity at this position, where magnetic scattering contributes only very weakly, differs somewhat from that measured previously with neutrons<sup>4</sup> at the (2, 1.5, 0) position where nuclear and magnetic reflections are superposed. The intensity of the equivalent (2, 1.5, 0) reflection of the same sample was also measured by X-ray diffraction (which is only sensitive to the lattice structure and not to the magnetic moments). Whereas the high-temperature ( $T \geq 40 \text{ K}$ ) portion of the curve of Fig. 1 was reproduced with X-rays, a surprising effect occurred at lower temperatures. Figure 2 shows that the intensity of the reflection decreases continuously with X-ray illumination; no change is observed when the X-ray beam is switched off. The diminution of the charge order is associated with a dramatic change in transport properties. The conductance measured between two contacts spaced  $\sim 1 \text{ mm}$  apart on a polished surface of the sample increases by more than six orders of magnitude after  $\sim 20 \text{ min}$  of total X-ray exposure (Fig. 2). With the X-ray beam off, the conductivity persists for many hours without measurable degradation.

Although the metallic state generated after prolonged X-ray exposure exhibits conventional ohmic conductivity (Fig. 3b), Fig. 3a shows that the current-voltage characteristics after short exposure are remarkably nonlinear. (We have therefore quoted conductance rather than conductivity in Fig. 2). The non-ohmic conductivity in this regime is a consequence of a much more general current switching behaviour which will be discussed separately. We obtain  $\rho \approx 5 \times 10^{-4} \text{ \Omega cm}$  for the ohmic resistivity after prolonged X-ray exposure, using the calculated X-ray penetration depth of  $1.5 \text{ \mu m}$  as the depth of the conducting channel between the contacts. This is (to within the errors) identical to the resistivity measured without X-rays above the critical magnetic field<sup>3</sup>, suggesting that the photoinduced and field-induced metallic phases are identical.

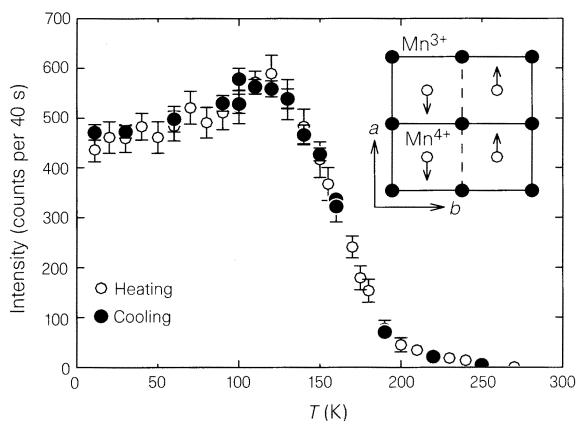


**Figure 1** Intensity of a (4, 1.5, 0) superlattice reflection characteristic of the low-temperature charge ordered state of  $\text{Pr}_{0.7}\text{Ca}_{0.3}\text{MnO}_3$ , measured by neutron diffraction on a single-crystal sample. The crystal was grown by the floating zone technique, details of which are given in ref. 3. The measurements were taken on the H7 spectrometer at the High Flux Beam Reactor, Brookhaven National Laboratory, with 14.7-meV neutrons. The filled (open) symbols represent data taken on cooling (heating). The inset shows a two-dimensional section of the charge-ordering pattern with the primary lattice distortion.

Further strong evidence for this assertion comes from a comparison of the metastability boundaries of these two metallic states. Figure 4 shows that the X-ray-induced conductivity is annealed out on heating above 60 K, which is the annealing temperature for the magnetic-field-induced phase<sup>3</sup>. Figure 2 also shows phase coexistence of the insulating (charge-ordered) and metallic states for short exposures which may indicate that the photoinduced transition is first order, as is the field-induced transition<sup>3</sup>. We have also repeated our X-ray measurements in magnetic fields up to  $H_c$  and find that the photoinduced transition occurs faster under these conditions. Though the magnetization was not measured directly, the close analogy to the magnetic-field-induced transition implies that the magnetic properties of the sample change dramatically with illumination, from canted antiferromagnetic to ferromagnetic. To our knowledge, a photoinduced antiferromagnetic-to-ferromagnetic transition has thus far not been observed.

We have considered several possible mechanisms for the observed photoinduced transition. First, photoinduced oxygen diffusion has been implicated in photoconductivity in some layered and amorphous oxides with very large oxygen mobilities<sup>11,12</sup>, but cannot play a role in this cubic material. An oxygen-diffusion mechanism is also ruled out by the above comparison of photoinduced and magnetic-field-induced transitions. Further, beam heating cannot be responsible because the conductivity and the Bragg peak intensity do not recover when the beam is switched off. We thus conclude that the increased conductivity is caused by X-ray photoelectrons and secondary electrons generated in collisions.

Significant transient X-ray photocurrents have been observed in a variety of materials such as amorphous Se (ref. 13), but to our knowledge persistent X-ray photoconductivity has not yet been reported. To explain why the X-ray-generated carriers are not recaptured when the beam is switched off, it helps to recall models for persistent (visible-light) photoconductivity in III-V semiconductors in the presence of DX centres<sup>14,15</sup>. These centres are thought to be associated with large lattice distortions which can be thermally excited at high temperatures, resulting in trapping of charge carriers. When carriers are photoexcited out of the traps at low temperatures, however, the lattice relaxes and the capture cross-section (mediated only by zero-point fluctuations of the lattice) becomes extremely small. Despite the different photon energies

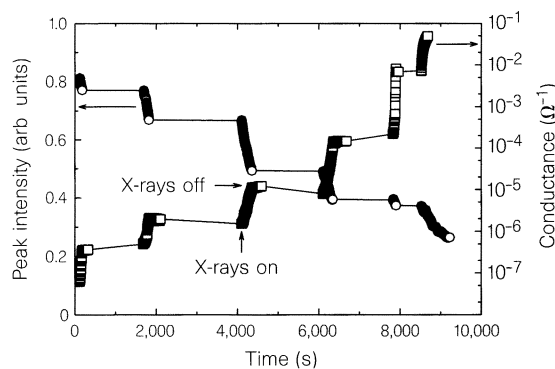


**Figure 2** X-ray exposure dependence of the peak intensity of the (2, 1.5, 0) Bragg reflection characteristic of charge ordering (left axis), and of the electrical conductance (right axis), at temperature  $T = 4 \text{ K}$ . The measurements were taken with a monochromatic X-ray beam (energy 8 keV, flux  $5 \times 10^{10} \text{ s}^{-1}$ , beam size  $1 \times 1 \text{ mm}$ ) at beamline X22B, National Synchrotron Light Source.

used in the experiments, the phenomenology of DX centres, including in particular the annealing of the metastable conducting state at elevated temperatures, bears a striking resemblance to our observations in  $\text{Pr}_{0.7}\text{Ca}_{0.3}\text{MnO}_3$ .

These observations have important implications both for the mechanism of colossal magnetoresistance (CMR) and for the physics of persistent photoconductivity in general. One of the most perplexing aspects of the physical properties of the manganites is their insulating state; traditional models of these materials cannot account

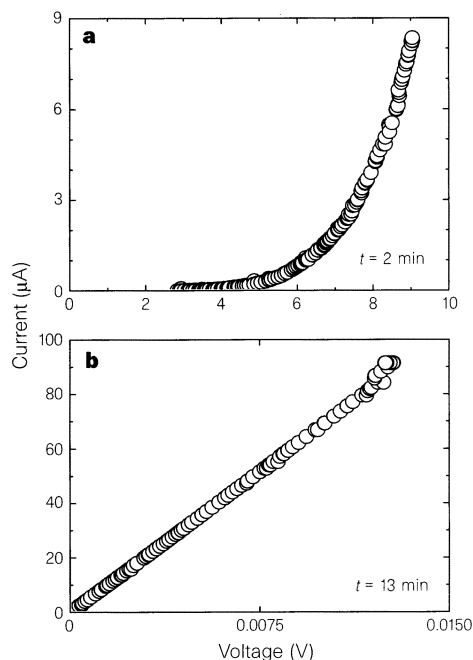


**Figure 3** Current-voltage characteristics measured after different X-ray exposures at temperature  $T = 4\text{ K}$ .

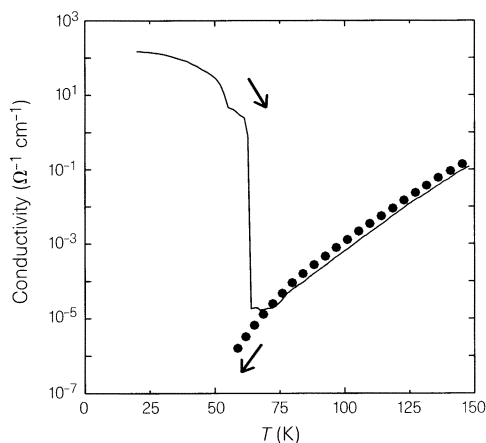


**Figure 4** Conductivity measured on cooling before X-ray illumination (dotted curve) and on heating after illumination with X-rays for a moderate amount of time (solid curve). In the unilluminated state, the conductivity was measured directly and is consistent with the measurements of ref. 3. X-ray illumination creates a conducting channel of depth equal to the X-ray penetration depth ( $\sim 1.5\ \mu\text{m}$ ) between two contacts spaced  $\sim 1\text{ mm}$  apart on a polished surface of the sample. Conductance data taken in the illuminated, unannealed state at low temperatures were converted to conductivity by using the calculated channel depth.

for this<sup>6</sup>. Current theories of CMR<sup>6</sup> therefore invoke strong polaronic self-trapping of the carriers mediated by the Jahn–Teller distortion of the  $\text{Mn}^{3+}$  ion. In conjunction with the DX centre analogy, our data clearly illustrate the dominant role of electron–lattice coupling as a driving force for charge localization and suggest that the insulating state in  $\text{Pr}_{0.7}\text{Ca}_{0.3}\text{MnO}_3$  should be regarded as a polaron lattice. Conversely, the lattice distortions around DX centres have thus far not been observed directly, which leaves a gap in an otherwise reasonably complete understanding of persistent photoconductivity. This gap is filled by the diffraction data of Fig. 2 which demonstrate unambiguously that the lattice relaxes when photoelectrons are removed from the charge-ordered state of  $\text{Pr}_{0.7}\text{Ca}_{0.3}\text{MnO}_3$ . The large relaxation of the lattice on entering the same metallic state through two different routes (X-rays and magnetic field) also provides a common microscopic explanation of the newly discovered persistent photoconductivity and the irreversibility effects observed in previous magnetotransport experiments on  $\text{Pr}_{0.7}\text{Ca}_{0.3}\text{MnO}_3$  and other manganites<sup>3,5</sup>.

The initial experiments reported here open the way for a variety of further experimental studies. For instance, further insight into the mechanism of the photoinduced transition could be gained by studying its dependence on photon energy. Preliminary experiments show that the kinetics of the transition are not strongly affected when the X-ray energy is lowered below the Mn K absorption edge, which may indicate that these phenomena occur over a wide energy range. From the point of view of applications, the unique properties of the manganites may, with further development, prove useful in X-ray lithography and X-ray detection. Perhaps even more importantly, the evidence presented here strongly suggests that the photoinduced phase is not only metallic but also ferromagnetic. Using X-ray lithography it should thus be feasible to pattern very small ferromagnetic structures into these materials, which would open up new possibilities for both fundamental and applied research on magnetism. In a compound of slightly modified composition,  $\text{Pr}_{0.65}\text{Ca}_{0.245}\text{Sr}_{0.105}\text{MnO}_3$ , we have recently observed significant persistent X-ray photoconductivity at temperatures in excess of 100 K, an important step towards practicability of these ideas. □

Received 8 October 1996; accepted 10 March 1997.

- Chahara, S., Ohno, T., Kasai, K. & Kozono, Y. Magnetoresistance in magnetic manganese oxide with intrinsic antiferromagnetic spin structure. *Appl. Phys. Lett.* **63**, 1990–1992 (1993).
- Lin, S. *et al.* Thousandfold change in resistivity in magnetoresistive La–Ca–Mn–O films. *Science* **264**, 413–415 (1994).
- Tomioka, Y., Asamitsu, A., Kuwahara, H., Moritomo, Y. & Tokura, Y. Magnetic-field-induced metal-insulator phenomena in  $\text{Pr}_{1-x}\text{Ca}_x\text{MnO}_3$  with controlled charge-ordering instability. *Phys. Rev. B* **53**, R1689–R1692 (1996).
- Yoshizawa, H., Kawano, H., Tomioka, Y. & Tokura, Y. Neutron-diffraction study of the magnetic-field-induced metal-insulator transition in  $\text{Pr}_{0.7}\text{Ca}_{0.3}\text{MnO}_3$ . *Phys. Rev. B* **52**, R13145–R13148 (1995).
- Tokura, Y., Kuwahara, H., Moritomo, Y., Tomioka, Y. & Asamitsu, A. Competing instabilities and metastable states in  $(\text{Nd}, \text{Sm})_{1-x}\text{Sr}_x\text{MnO}_3$ . *Phys. Rev. Lett.* **76**, 3184–3187 (1996).
- Millis, A. J., Littlewood, P. M. & Shraiman, B. I. Double exchange alone does not explain the resistivity of  $\text{La}_{1-x}\text{Sr}_x\text{MnO}_3$ . *Phys. Rev. Lett.* **74**, 5144–5147 (1995).
- Park, J. H. *et al.* Electronic aspects of the ferromagnetic transition in manganese perovskites. *Phys. Rev. Lett.* **76**, 4215–4218 (1996).
- Billinge, S. J. L., Difrancesco, R. G., Kwei, G. H., Neumeier, J. J. & Thomson, J. D. Direct observation of lattice polaron formation in the local structure  $\text{La}_{1-x}\text{Ca}_x\text{MnO}_3$ . *Phys. Rev. Lett.* **77**, 715–718 (1996).
- Shenglaya, A., Zhao, G. M., Keller, H. & Müller, K. A. EPR-evidence of Jahn–Teller polaron formation in  $\text{La}_{1-x}\text{Ca}_x\text{MnO}_{3.1}$ . *Phys. Rev. Lett.* **77**, 5296–5299 (1996).
- Jirak, Z., Krupicka, S., Simsa, Z., Dlouha, M. & Vratislav, S. Neutron diffraction study of  $\text{Pr}_{1-x}\text{Ca}_x\text{MnO}_3$  perovskites. *J. Magn. Magn. Mat.* **53**, 153–166 (1985).
- Pashmakov, B., Claflin, B. & Fritzsche, H. Photoreduction and oxidation of amorphous indium oxide. *Solid State Commun.* **86**, 619–622 (1993).
- Kudinov, V. I. *et al.* Persistent photoconductivity in  $\text{YBa}_2\text{Cu}_3\text{O}_{7-x}$  films as a method of photodoping toward metallic and superconducting phases. *Phys. Rev. B* **47**, 9017–9028 (1993).
- Donovan, J. L. X-ray sensitivity of selenium. *J. Appl. Phys.* **50**, 6500–6554 (1979).
- Mooney, P. M. Deep donor levels (DX centers) in III–V semiconductors. *J. Appl. Phys.* **67**, R1–R26 (1990).
- Lang, D. V. in *Deep Centres in Semiconductors* (ed. Pantelides, S. T.) 489–539 (Gordon & Breach, New York, 1986).

**Acknowledgements.** We thank B. L. Altshuler, P. W. Anderson, D. A. Huse, H. M. Jaeger, N. P. Ong and J. M. Tranquada for discussions. The work at Princeton University was supported by the US NSF and by the Packard and Sloan foundations; the work at Brookhaven National Laboratory was supported by the US Department of Energy; this work was also supported in part by NEDO and by the Ministry of Education, Japan.

Correspondence and requests for materials should be addressed to B.K.